

See discussions, stats, and author profiles for this publication at: <https://www.researchgate.net/publication/236062309>

Intein-Triggered Artificial Protein Hydrogels That Support the Immobilization of Bioactive Proteins

ARTICLE in JOURNAL OF THE AMERICAN CHEMICAL SOCIETY · MARCH 2013

Impact Factor: 12.11 · DOI: 10.1021/ja401075s · Source: PubMed

CITATIONS

17

READS

74

4 AUTHORS, INCLUDING:



Miguel Ramirez

University of Otago

5 PUBLICATIONS 56 CITATIONS

SEE PROFILE



Dongli Guan

Texas A&M University

8 PUBLICATIONS 69 CITATIONS

SEE PROFILE



Zhilei Chen

Texas A&M University

26 PUBLICATIONS 558 CITATIONS

SEE PROFILE

Intein-Triggered Artificial Protein Hydrogels That Support the Immobilization of Bioactive Proteins

Miguel Ramirez,[†] Dongli Guan,[†] Victor Ugaz,[†] and Zhilei Chen^{*,†,‡}[†]Artie McFerrin Department of Chemical Engineering, Texas A&M University, and [‡]Department of Microbial and Molecular Pathogenesis, Texas A&M Health Science Center, College Station, Texas 77843, United States

S Supporting Information

ABSTRACT: Protein hydrogels have important applications in tissue engineering, drug delivery, and biofabrication. We present the development of a novel self-assembling protein hydrogel triggered by mixing two soluble protein block copolymers, each containing one half of a split intein. Mixing these building blocks initiates an intein trans-splicing reaction that yields a hydrogel that is highly stable over a wide range of pH (6–10) and temperature (4–50 °C), instantaneously recovers its mechanical properties after shear-induced breakdown, and is compatible with both aqueous and organic solvents. Incorporating a “docking station” peptide into the hydrogel building blocks enables simple and stable immobilization of docking protein-fused bioactive proteins in the hydrogel. This intein-triggered protein hydrogel technology opens new avenues for both in vitro metabolic pathway construction and functional/biocompatible tissue engineering scaffolds and provides a convenient platform for immobilizing enzymes in industrial biocatalysis.

Enzymes are versatile catalysts due to their superior chemo-, regio-, and stereospecificity. However, lack of long-term stability under process conditions and difficulties in recovery and recycling greatly hamper the usefulness of enzymes in industrial processes. Immobilization alleviates some of these limitations.¹ In most cases, to achieve stable immobilization, target enzymes need to be covalently linked to a supporting matrix through a chemical conjugation reaction involving the side-chain functionalities of the amino acids cysteine and lysine. The properties of the bioconjugates thus generated are influenced by the frequency and location of lysine/serine residues and are highly variable depending on the target enzyme.^{1b} Recently, a number of protein derivatization techniques to achieve site-specific protein immobilization have been developed, including expressed protein ligation,² Staudinger ligation,³ and “click” ligation.⁴ However, in view of the fact that it is often difficult to determine a priori which sites in a protein are essential for a function versus available for modification, there remains a major demand for the development of new and more general technologies for high-density, high-activity enzyme immobilization on solid supports.

Here we demonstrate the synthesis and application of a split-intein-triggered protein hydrogel as a general scaffold for enzyme immobilization. The split-intein-containing protein building blocks used are the copolymers CutA-*NpuN* (N) and *NpuC*-S-CutA (C) (Figure 1A and Table S1). *NpuN* and *NpuC* are the N

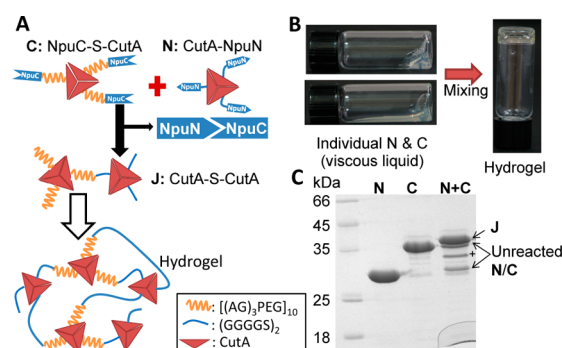


Figure 1. Intein-triggered protein hydrogel. (A) Schematic of intein trans-splicing reaction that triggers formation of an extended protein chain J with cross-linker proteins at both termini. Cross-linker proteins from multiple J chains noncovalently interact with each other upon intein-triggered protein ligation, forming a highly cross-linked protein network with hydrogel properties. *NpuN* and -C are the intein N and C fragments. (B) Mixing purified N and C (8.3% w/v) forms a highly cross-linked hydrogel network (1.6 mM J). (C) SDS-PAGE analysis of purified N and C building blocks before and after mixing. N+C corresponds to a sample taken directly from 1.6 mM hydrogel; + denotes an intein C-terminal cleavage side reaction product.

and C fragments of the naturally split DnaE intein from *Nostoc punctiforme* (*Npu*). We chose this intein for its extraordinarily quick reaction kinetics ($t_{1/2} = 63$ s) and very high trans-splicing yield (75–85%).⁵ CutA, a small trimeric protein (12 kDa) from *Pyrococcus horikoshii*, was used as the cross-linker protein.⁶ CutA has an extremely high denaturation temperature of nearly 150 °C and retains its trimeric quaternary structure in solutions with as much as 5 M GuHCl.^{6a} The ultrahigh stability of CutA is attributed to its very large number of intra- and intersubunit ionic pairs that form extensive ion-pair networks.⁷ We reasoned that the very strong intersubunit interactions should discourage subunit exchange between different cross-linkers, minimizing hydrogel surface erosion by forming closed loops.⁸ The S fragment, $[(AG)_3PEG]_{10}$,⁹ a flexible polyanionic linker, was incorporated as the midblock for water retention. Mixing N and C initiates a trans-splicing reaction between *NpuN* and *NpuC*, generating a longer protein chain with the cross-linker CutA at both termini. Cross-linkers from multiple molecular units of this type interact with each other, forming a highly cross-linked gel-like network (Figure 1A).

Received: January 30, 2013

Published: March 20, 2013

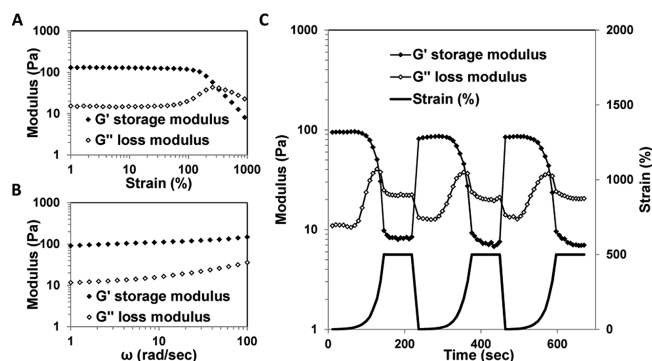


Figure 2. Rheological characterization of a hydrogel with 1.6 mM J. (A) Strain sweep at 10 rad/s. (B) Angular frequency sweep at 10% strain. (C) LAOS cycles at 10 rad/s.

For hydrogel formation, purified N and C were manually mixed at a 1:1 molar ratio via a swirling motion using a pipet tip in Dulbecco's phosphate-buffered saline (DPBS) supplemented with 5 mM dithiothreitol (DTT) (buffer E in Table S3). DTT activates the intein trans-splicing reaction between N and C,¹⁰ triggering formation of protein fragment CutA-S-CutA (J) (Figure 1A,C). However, due to the very high affinity between the intein N and C fragments, the hydrogel can also form in the absence of DTT. The final concentration of cross-linked protein J was ~5% w/v (combined mass of N and C minus that of the spliced inteins), or 1.6 mM. Individually, the N and C proteins were viscous liquids, but when the fragments were mixed, a gel-like material formed (Figure 1B). Densitometric analysis of SDS-PAGE gels revealed that ~80% of the input protein successfully underwent the trans-splicing reaction (Figure 1C).

The gel-like material formed upon mixing N and C was confirmed to be a hydrogel by rheological analysis, which showed a substantially greater plateaued storage modulus (G') relative to the loss modulus (G'') over a wide range of frequencies and strains (Figure 2A,B). An intein-triggered hydrogel with 1.6 mM J retained its elastic properties at ~100% strain amplitude (Figure 2A). At strains above 100%, G' decreased while G'' increased until the two values crossed each other and the hydrogel transitioned from a predominantly elastic material to a viscous fluid. The increase in energy dissipation seen in G'' at this transition point suggests disruption of noncovalent associations within the network,¹¹ likely involving dissociation of CutA trimers into monomers. The G'_{∞} plateau value for a hydrogel with 1.6 mM J was 110 ± 27 Pa. Measurements were made on three separate samples, and the reported errors are standard deviations. The hydrogel mechanical properties are influenced by the choice of both cross-linker and midblock.¹¹ The cross-linker structure governs the number of intermolecular interactions in the hydrogel. Previously it was shown that a hydrogel with tetrameric cross-linkers has lower G'_{∞} (~400 Pa) than one with pentameric cross-linkers (>1000 Pa).⁸ The trimeric cross-linker structure of this intein hydrogel may be partially responsible for the low G'_{∞} , and a higher G'_{∞} could be obtained by using a different cross-linker protein with a higher order of multimerization.

Dynamic rheological characterization revealed that our intein-triggered hydrogel instantaneously recovers its mechanical properties after shear-induced breakdown (Figure 2C). A small but permanent loss of elastic modulus (10%) was seen after the first cycle of large-amplitude oscillatory shear (LAOS). However, G' did not decrease further in subsequent LAOS cycles. The very rapid recovery kinetics is attributed to the use of a single protein,

CutA, as the cross-linker, allowing the disengaged monomers to associate very easily with other monomers to reform new trimeric cross-linkers. Hydrogels with nonsymmetrical cross-linkers typically exhibit slower recovery kinetics.¹² The ability of the intein-triggered hydrogel to recover its mechanical properties after LAOS points to the injectability of this hydrogel, which is highly desirable for controlled drug delivery and tissue engineering.¹³

The intein-triggered protein hydrogel (1.6 mM J) exhibited remarkable stability in aqueous solution. After 21 days at 22 °C, the total amount of protein released into the solution only slightly exceeded the theoretical amount of the spliced-out intein (calculated based on 100% trans-splicing efficiency), indicating little to no loss of the cross-linked hydrogel scaffold (Figure 3A).

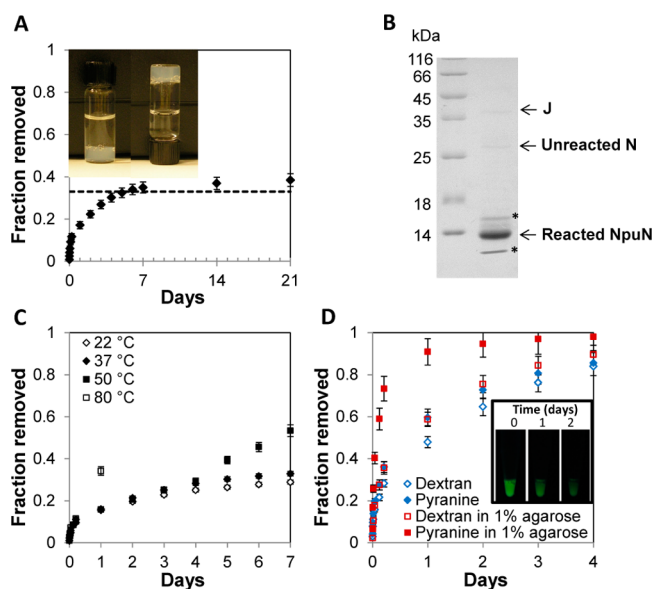


Figure 3. Stability of intein-triggered hydrogels in DPBS. (A) Erosion of a 1.6 mM hydrogel at 22 °C. The dashed line represents the theoretical mass corresponding to the cleaved inteins. Inset: undisturbed hydrogel in DPBS after 3 months at rt. (B) SDS-PAGE analysis of the buffer surrounding the hydrogel. All the samples of the buffer in which the hydrogel was immersed in (A) were pooled (7.5 mL total) and concentrated 75-fold via ultrafiltration through a 10 kDa membrane before gel loading. J, intein trans-spliced product; N, CutA-NpuN; NpuN, spliced-out NpuN. Unreacted C and spliced-out NpuC are not visible in the gel due to their small quantity and size (4 kDa), respectively. Asterisks denote unidentified bands. (C) Erosion profile of hydrogels incubated at different temperatures. (D) Diffusion kinetics of FITC-dextran (20 kDa) and pyranine (524 Da) from 1.6 mM hydrogels and 1% agarose gels. Inset: hydrogel containing pyranine under UV exposure at three time points. Error bars represent SD of two independent experiments.

SDS-PAGE analysis confirmed this result, showing only trace amounts of the trans-spliced product in the surrounding buffer (Figure 3B, band J). The vast majority of the protein in the surrounding buffer was spliced intein that diffused out of the hydrogel. The hydrogel volume expanded significantly in the first 24 h and slightly in the first week as a result of hydrogel swelling but did not detectably change after that, likely because loss of cross-linked hydrogel scaffold was negligible. An undisturbed hydrogel was stable in aqueous solution at room temperature (rt) for over 3 months with essentially no erosion (Figure 3A inset). Small isolated air bubbles that occasionally became trapped at the hydrogel surface during hydrogel formation remained after 3

months, indicating the hydrogel did not undergo surface erosion due to closed loop formation.^{8,14}

We next determined the stability of this hydrogel under various conditions. The hydrogel exhibited similar erosion profiles in pH 6.0 and 10.0 buffers (Figure S1A), and a hydrogel with as little as 0.8 mM J (2.7% w/v) retained ~40% of its initial mass after 7 days in DPBS buffer at rt (Figure S1B). The hydrogel was also stable at 37 °C but less so at 50 °C (Figure 3C). The elevated hydrogel erosion rate at high temperatures is somewhat surprising since CutA retains its trimeric quaternary structure up to 150 °C.^{6a} It is possible that high temperature increases the vibrational motion of the S fragment, resulting in temporary separation of the CutA trimers. The hydrogel stability might be further improved by introducing covalent linkages (e.g., disulfide bonds) into the CutA trimer.

For our intein hydrogel, the normalized plateau storage modulus G'_{∞}/nkT (where n is the chain number density, k Boltzmann's constant, and T absolute temperature) was only 0.024, indicating that most of the cross-linkers were not productively connected and that the hydrogel contained a large number of independent loops.⁸ Since the intein-triggered hydrogel exhibited little to no surface erosion, one possible reason for the low magnitude of G'_{∞} was hydrogel inhomogeneity due to manual mixing. Since the *Npu* intein has very rapid reaction kinetics ($t_{1/2} = 63$ s), the interface between the N and C solutions may rapidly react to form hydrogel "sheets" with a high level of cross-linking, while regions away from the interface may be connected by a smaller number of intermolecular interactions. The bulk rheology experiments measure the lowest storage modulus (i.e., the "weakest link") in a material, which may explain why our hydrogel exhibited a low overall G'_{∞} value. Formation of hydrogel sheets is supported by the observation that our intein hydrogel crumbled into small sheetlike structures when incubated in DPBS at elevated temperature (>50 °C) during the erosion experiment. This phenomenon also suggests that the mechanical properties of the hydrogel could be tuned over a wide range by controlling the mixing rate.

Molecules of <20 kDa easily diffused out of the hydrogel (Figure 3D). However, small (pyranine, 534 Da) and large (20 kDa dextran) molecules appeared to diffuse out of the hydrogel at similar rates. In contrast, agarose gels showed a much higher diffusion rate for pyranine than for dextran (Figure 3D). The pore size of our intein-triggered hydrogel is primarily governed by the size and physicochemical properties of the midblock chain. The average hydrodynamic diameter of the S fragment chain is 40 Å,¹⁵ and the diagonal distance of CutA trimer is ~45 Å (measured from PDB entry 1V99). The average pore size of this hydrogel is expected to be similar to the cytosolic environment.¹⁶ The similar diffusion rates for dextran and pyranine may reflect the dynamic nature of the hydrogel, in which molecular diffusion is limited by the vibrational motion of the S fragment. Use of a protein with an elongated or rigid structure as a midblock should yield an expanded hydrogel pore size, facilitating molecular diffusion.

Next, we tested the ability of the intein-triggered hydrogel to function as a protein immobilization scaffold. For this we chose the Src homology 3 domain from the adaptor protein CRK (SH3) and its ligand (SH3_{lig}) as the docking protein (DP) and docking station peptide (DSP), respectively, due to their relatively small size (56 and 11 amino acids, respectively), high affinity for each other ($K_d = 0.1 \mu\text{M}$),¹⁷ and previous application in intracellular protein docking.¹⁸ SH3_{lig} was inserted between S and CutA in C to form C-SH3_{lig} (Table S1). SH3 was fused to the

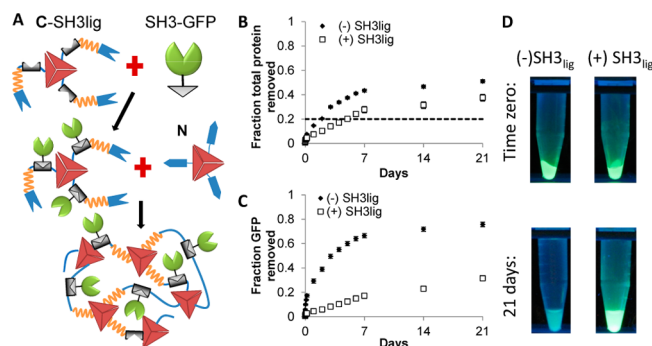


Figure 4. Intein-triggered hydrogel as a scaffold for protein immobilization. (A) Schematic of protein immobilization using GFP as a model globular protein. DSP-containing hydrogel building blocks are first mixed with DP-fused target protein. The complementary intein-fragment-containing hydrogel building block is then added to the mixture, yielding a hydrogel with immobilized GFP. (B) Total protein erosion profile of hydrogel with 1:1 molar ratio of SH3-GFP and C-SH3_{lig}. The dotted line represents the theoretical mass corresponding to the spliced-out inteins. Error bars represent SD of two independent experiments. (C) Leaching profile of SH3-GFP from hydrogels with and without DSP. (D) Images of GFP-containing hydrogels under UV exposure immediately after and 21 days after hydrogel formation.

N-terminus of green fluorescent protein (GFP) to form SH3-GFP. Purified C-SH3_{lig} and SH3-GFP were mixed in a 1:1 molar ratio to facilitate docking SH3 to SH3_{lig}. An equimolar amount of N was then added to form a hydrogel with embedded GFP (Figure 4A). The final hydrogel contained 1.2 mM trans-spliced hydrogel backbone and 1.2 mM GFP (SH3-GFP/C-SH3_{lig}/N molar ratio of 1:1:1). Incorporating GFP did not compromise the hydrogel's stability in solution (Figures 4B and S2). Leaching of immobilized SH3-GFP from SH3_{lig}-containing hydrogel was ~30% after 3 weeks, significantly less than that from a hydrogel lacking SH3_{lig}, which lost >70% of the entrapped protein within the same period (Figure 4C). The immobilized SH3-GFP in the hydrogel could be conveniently visualized under UV light, and the SH3_{lig}-containing hydrogel retained most of the GFP fluorescence after 3 weeks, while the hydrogel lacking SH3_{lig} lost most of its fluorescence (Figure 4D). It is possible that an even lower leaching rate of immobilized protein could be achieved if a higher-affinity DP/DSP pair were used. It should be possible to immobilize any DP-fused target protein in a similar fashion. These results provide a first proof-of-principle that our intein-triggered protein hydrogel can be used as a general scaffold for protein immobilization through a method that does not significantly impact the protein activity: the docking of a protein–protein pair. This result is in contrast to the currently widely used method of chemical immobilization of proteins by modification of Cys and Lys side chains, which can negatively impact protein activity.^{1b}

The density of immobilized GFP in the current hydrogel was ~33 mol%. A higher immobilization density could be achieved by incorporating multiple DSP sites into the hydrogel building blocks. Docking target proteins onto individual hydrogel building blocks before hydrogel formation ensures an even distribution of target protein throughout the hydrogel. Since the identity and location of the DSP are genetically encoded, specific ordering and ratios of different proteins could be conveniently achieved by incorporating different DSPs in the hydrogel building block. This approach would also facilitate tuning multienzyme reaction cascades to achieve high in vitro reaction

rates and yields. Alternatively, the same hydrogel building block with a given DSP could be separately preloaded with different target proteins, and solutions of a hydrogel building block loaded with the different target proteins could be mixed at any desired ratio before adding the protein building block with the complementary split intein fragment. This second approach would enable convenient immobilization of different proteins at any desired ratio using a single DP/DSP pair, facilitating, e.g., convenient multienzyme metabolic pathway optimization *in vitro*.¹⁹

We next looked at the ability of our protein hydrogel to facilitate an enzymatic reaction in an organic solvent. Enzymes hold enormous potential as catalysts for organic synthesis, but they are rarely used for this purpose due to their low activity and stability in organic solvents.²⁰ Synthetic polymer hydrogels have been used to prevent enzyme denaturation in organic solvents.²¹ Using horseradish peroxidase (HRP) as the model enzyme and the oxidative coupling of *N,N*-dimethyl-*p*-phenylenediamine and phenol with *tert*-butyl hydroperoxide as the model reaction,²² we determined the ability of our hydrogel to protect the immobilized enzyme from the denaturing effect of the organic solvent, heptane. A hydrogel entrapping 0.042 mM HRP was immersed in heptane for 24, 9, or 0 h before adding reaction substrates. To increase the area of the hydrophilic/hydrophobic interface, this hydrogel was manually disrupted into small pieces after immersion in the solvent. As anticipated, HRP entrapped in the hydrogel catalyzed rapid oxidation reactions, giving rise to a colorimetric product that was quantifiable via spectrophotometry. The product accumulated linearly regardless of the amount of time in contact with the solvent, indicating little to no enzyme inactivation by heptane (Figure S3). In contrast, HRP added directly to heptane exhibited very low catalytic activity due to enzyme inactivation. HRP first dissolved in DPBS and then immersed in heptane for 24, 9, or 0 h was unable to catalyze significant conversion, likely due to the very limited surface area between the enzyme in the aqueous phase and the substrate in the organic phase. The ability of our protein hydrogel to withstand the denaturing effect of an organic solvent is attributed to incorporation of the hydrophilic S fragment in the hydrogel backbone, which effectively “locks” water molecules inside the hydrogel, preventing organic solvent from accessing the hydrogel interior. These results demonstrate the potential of our intein-triggered protein hydrogel as a scaffold for enzymatic reactions in organic solvents.

In summary, we have engineered a new protein hydrogel that conditionally assembles in response to a split-intein-triggered trans-splicing reaction. This hydrogel is formed under physiological conditions and shows unprecedented stability under a broad set of conditions. In addition, this intein-triggered hydrogel is compatible with cell culture growth medium (Figure S4), pointing to its potential for use as a scaffold for tissue engineering applications. The intein-triggered hydrogel technology provides a new platform for protein hydrogel design and synthesis and should find use in many research and biofabrication applications, including enzyme immobilization, bioelectrode fabrication, organic synthesis, injectable drug delivery, and functional tissue engineering scaffolds.

■ ASSOCIATED CONTENT

■ Supporting Information

Experimental details, tables of constructs and primers, and additional experimental data. This material is available free of charge via the Internet at <http://pubs.acs.org>.

■ AUTHOR INFORMATION

Corresponding Author

zchen4@tamu.edu

Notes

The authors declare no competing financial interest.

■ ACKNOWLEDGMENTS

This work was supported in part by NSF CAREER, U.S. Air Force YIP, and the Norman Hackman Advanced Research Program.

■ REFERENCES

- (1) (a) Mateo, C.; Palomo, J. M.; Fernandez-Lorente, G.; Guisan, J. M.; Fernandez-Lafuente, R. *Enzyme Microb. Technol.* **2007**, *40*, 1451. (b) Sheldon, R. A. *Adv. Synth. Catal.* **2007**, *349*, 1289.
- (2) Muralidharan, V.; Muir, T. W. *Nat. Methods* **2006**, *3*, 429.
- (3) Kalia, J.; Abbott, N. L.; Raines, R. T. *Bioconjugate Chem.* **2007**, *18*, 1064.
- (4) (a) Weikart, N. D.; Mootz, H. D. *ChemBioChem* **2010**, *11*, 774. (b) Wieczorek, B.; Lemcke, B.; Dijkstra, H. P.; Egmond, M. R.; Gebbink, R. J. M. K.; van Koten, G. *Eur. J. Inorg. Chem.* **2010**, 1929.
- (5) (a) Zettler, J.; Schutz, V.; Mootz, H. D. *FEBS Lett.* **2009**, *583*, 909. (b) Carvajal-Vallejos, P.; Pallisse, R.; Mootz, H. D.; Schmidt, S. R. *J. Biol. Chem.* **2012**, *287*, 28686.
- (6) (a) Tanaka, Y.; Tsumoto, K.; Nakanishi, T.; Yasutake, Y.; Sakai, N.; Yao, M.; Tanaka, I.; Kumagai, I. *FEBS Lett.* **2004**, *556*, 167. (b) Sawano, M.; Yamamoto, H.; Ogasahara, K.; Kidokoro, S.; Katoh, S.; Ohnuma, T.; Katoh, E.; Yokoyama, S.; Yutani, K. *Biochemistry* **2008**, *47*, 721.
- (7) Tanaka, T.; Sawano, M.; Ogasahara, K.; Sakaguchi, Y.; Bagautdinov, B.; Katoh, E.; Kuroishi, C.; Shinkai, A.; Yokoyama, S.; Yutani, K. *FEBS Lett.* **2006**, *580*, 4224.
- (8) Shen, W.; Zhang, K.; Kornfield, J. A.; Tirrell, D. A. *Nat. Mater.* **2006**, *5*, 153.
- (9) (a) McGrath, K. P.; Fournier, M. J.; Mason, T. L.; Tirrell, D. A. *J. Am. Chem. Soc.* **1992**, *114*, 727. (b) Petka, W. A.; Harden, J. L.; McGrath, K. P.; Wirtz, D.; Tirrell, D. A. *Science* **1998**, *281*, 389.
- (10) (a) Ramirez, M.; Valdes, N.; Guan, D.; Chen, Z. *Protein Eng., Des. Sel.* **2013**, *26*, 215. (b) Mohlmann, S.; Bringmann, P.; Greven, S.; Harrenga, A. *BMC Biotechnol.* **2011**, *11*, 76.
- (11) Olsen, B. D.; Kornfield, J. A.; Tirrell, D. A. *Macromolecules* **2010**, *43*, 9094.
- (12) Skrzyszewska, P. J.; Sprakel, J.; de Wolf, F. A.; Fokkink, R.; Stuart, M. A. C.; van der Gucht, J. *Macromolecules* **2010**, *43*, 3542.
- (13) (a) Yu, L.; Ding, J. D. *Chem. Soc. Rev.* **2008**, *37*, 1473. (b) Lu, H. D.; Charati, M. B.; Kim, I. L.; Burdick, J. A. *Biomaterials* **2012**, *33*, 2145.
- (14) Shen, W.; Kornfield, J. A.; Tirrell, D. A. *Macromolecules* **2007**, *40*, 689.
- (15) Shen, W. Ph.D. Dissertation, California Institute of Technology, Pasadena, CA, 2005.
- (16) (a) Novak, I. L.; Kraikivski, P.; Slepchenko, B. M. *Biophys. J.* **2009**, *97*, 758. (b) Svitkina, T. M.; Verkhovsky, A. B.; McQuade, K. M.; Borisy, G. G. *J. Cell Biol.* **1997**, *139*, 397.
- (17) Nguyen, J. T.; Turck, C. W.; Cohen, F. E.; Zuckermann, R. N.; Lim, W. A. *Science* **1998**, *282*, 2088.
- (18) Dueber, J. E.; Wu, G. C.; Malmirchegini, G. R.; Moon, T. S.; Petzold, C. J.; Ullal, A. V.; Prather, K. L.; Keasling, J. D. *Nat. Biotechnol.* **2009**, *27*, 753.
- (19) Jung, G. Y.; Stephanopoulos, G. *Science* **2004**, *304*, 428.
- (20) Schmid, A.; Dordick, J. S.; Hauer, B.; Kiener, A.; Wubbolts, M.; Witholt, B. *Nature* **2001**, *409*, 258.
- (21) (a) Liszka, M. J.; Clark, M. E.; Schneider, E.; Clark, D. S. *Annu. Rev. Chem. Biomol. Eng.* **2012**, *3*, 77. (b) Iyer, P. V.; Ananthanarayan, L. *Process Biochem.* **2008**, *43*, 1019.
- (22) Bruns, N.; Tiller, J. C. *Nano Lett.* **2005**, *5*, 45.